Published in final edited form as:
Prog Biophys Mol Biol. 2012 October ; 110(2-3): 372–379. doi:10.1016/j.pbiomolbio.2012.07.009.

A COMPUTATIONAL APPROACH TO UNDERSTANDING THE CARDIAC ELECTROMECHANICAL ACTIVATION SEQUENCE IN THE NORMAL AND FAILING HEART, WITH TRANSLATION TO THE CLINICAL PRACTICE OF CRT

Jason Constantino, **Yuxuan Hu**, and **Natalia A. Trayanova**
Baltimore, MD, Johns Hopkins University Department of Biomedical Engineering and the Institute of Computational Medicine

Abstract

Cardiac resynchronization therapy (CRT) is an established clinical treatment modality that aims to recoordinate contraction of the heart in dyssynchrous heart failure (DHF) patients. Although CRT reduces morbidity and mortality, a significant percentage of CRT patients fail to respond to the therapy, reflecting an insufficient understanding of the electromechanical activity of the DHF heart. Computational models of ventricular electromechanics, are now poised to fill this knowledge gap and provide a comprehensive characterization of the spatiotemporal electromechanical interactions in the normal and DHF heart. The objective of this paper is to demonstrate the powerful utility of computational models of ventricular electromechanics in characterizing the relationship between the electrical and mechanical activation in the DHF heart, and how this understanding can be utilized to devise better CRT strategies. The computational research presented here exploits knowledge regarding the three dimensional distribution of the electromechanical delay, defined as the time interval between myocyte depolarization and onset of myofiber shortening, in determining the optimal location of the LV pacing electrode for CRT. The simulation results shown here also suggest utilizing myocardial efficiency and regional energy consumption as a guide to optimize CRT.

Keywords

electromechanics; cardiac resynchronization therapy; whole-heart modeling; dyssynchronous heart failure

1. Introduction

Heart failure is a major cause of morbidity and mortality, contributing significantly to global health expenditure (Lloyd-Jones et al., 2009). Heart failure patients often exhibit contractile dyssynchrony, which diminishes cardiac systolic function. Cardiac resynchronization

Corresponding Author: Dr. Natalia Trayanova Department of Biomedical Engineering and Institute for Computational Medicine Johns Hopkins University 3400 N. Charles St. Hackerman Hall Room 216 Baltimore, MD 21218 ntrayanova@jhu.edu.

Disclosures NAT is a cofounder of CardioSolv, LLC. CardioSolv was not involved in this research.

therapy (CRT), a treatment modality that employs bi-ventricular (bi-V) pacing to re-coordinate the contraction of the heart, is a valuable therapeutic option for such patients (Linde et al., 2002). CRT has been shown to improve heart failure symptoms and reduce episodes of hospitalization, yet approximately 30% of patients fail to respond to the therapy (Abraham et al., 2002). The poor predictive ability of current approaches to identify potential responders to CRT reflects the incomplete understanding of the complex pathophysiologic and electromechanical factors that need to be considered to achieve optimal resynchronization in each dyssychronous heart. The objective of this paper is to demonstrate the important utility of computational models of ventricular electromechanics in providing a new level of understanding of the relationship between electrical and mechanical activation in the heart, and how this understanding can be utilized to devise better CRT strategies.

1.1 Dyssynchronous Heart Failure

Heart failure is characterized with impaired pump function due to the deleterious remodeling of the ventricles, from the organ down to the molecular level, which significantly alters the electrical and mechanical behavior of the heart. High-resolution magnetic resonance imaging (MRI) and diffusion tensor (DT) MRI scans (Helm et al., 2006) have shown that in DHF there is a substantial remodeling of ventricular geometry and structure. At the organ level, the ventricles become dilated and wall thickness is reduced. At the tissue level, laminar sheet angle is altered, and the transmural gradient in fiber orientation is increased. Because chamber geometry and sheet structure are major determinants of LV mechanics (Cheng et al., 2008; LeGrice et al., 1995), the mechanical deformation of the failing heart is markedly different. Furthermore, given the fact that fiber and sheet orientations directly influence the global 3D electrical activity of the normal heart (Hooks et al., 2007), it is conceivable that the altered geometry and fiber/sheet architecture in the failing heart will affect the 3D electrical propagation.

Heart failure is also characterized with remodeling of the electrophysiological and mechanical properties at the cellular and subcellular levels. Animal studies (Akar et al., 2007; Akar et al., 2004) have shown that the gap junctional protein connexin43 (Cx43) is redistributed from the intercalated disk to the lateral myocyte borders and that the amount of hypophosphorylated Cx43 is increased, leading to reduced conduction velocity in heart failure. There is a considerable downregulation of the membrane potassium channels carrying the Ito and IK1 currents (Kaab et al., 1996) and of the intracellular Ca2+ ATPase (SERCA) pump (O'Rourke et al., 1999), and upregulation of the Na–Ca exchanger (NCX) (O'Rourke et al., 1999). Remodeled ionic currents and Ca2+ handling result in altered Ca2+ transients, which, in turn, impair active tension development by the myofilaments in the cell. Finally, differential expression of collagen isoforms (Marijianowski et al., 1995) and altered ratio of titin (Wu et al., 2002) (an intrasarcomeric protein that modulates myofilament passive tension) isoforms results in increased myocardial stiffness.

Because of the combined effects of chamber, contractile, and electrophysiological remodeling, the ability of the LV to efficiently pump blood is severely compromised in heart failure patients. Furthermore, a subset of these patients exhibits abnormal electrical conduction that delays activation of one portion of the ventricle relative to another (intraventricular conduction delay due to left bundle branch block, LBBB). This results in contractile dyssynchrony (dyssynchronous heart failure, DHF), which further diminishes cardiac systolic function and energetic efficiency.

1.2. Cardiac Resynchronization Therapy

CRT is an established therapy for DHF patients. CRT typically employs bi-V pacing, with an endocardial right ventricular (RV) pacing lead and an epicardial LV pacing lead, to re-coordinate contraction (Bleeker et al., 2006a). CRT has been shown to acutely and chronically improve systolic function (Nelson et al., 2000) of the heart and to reverse the detrimental remodeling (Sutton et al., 2006) associated with heart failure.

Although CRT reduces morbidity and mortality, approximately 30% of patients fail to respond to the therapy. This reflects the poor predictive capability of current approaches to identify potential responders to CRT. The QRS duration (QRS ≥150 ms), widely used in clinical trials as a basic component of the inclusion criteria for CRT, does not provide an indication of the degree of mechanical dyssynchrony (Fauchier et al., 2003). Indeed, patients with long QRS duration may not exhibit mechanical dyssynchrony and those with short QRS complexes may present with significant dyssynchrony in contraction (Auricchio et al., 1999; Fauchier et al., 2002; Pitzalis et al., 2002). Measurements of mechanical dyssynchrony by tissue Doppler echocardiography (Bax et al., 2004; Yu et al., 2002) reveal only local dyssynchrony, while the complex deformations in DHF are global. The stress and strain distributions are heterogeneous throughout the DHF heart (Byrne et al., 2007; Helm et al., 2005; Kerckhoffs et al., 2011), and echocardiographic indices do not reflect the non-uniformity of strain since they account for the local deformation only. In recent clinical trials, Doppler echocardiography was characterized by lack of reproducibility and low predictive value (Beshai et al., 2007; Chung et al., 2008; Miyazaki et al., 2010). The poor predictive capability of the above measures indicates an incomplete understanding of the relation between the electrical and mechanical events in DHF.

The presence of myocardial infarction (MI) is an additional reason for lack of response to CRT. Placement of a pacing electrode at or near the infarct scar may result in ineffective pacing and thus in failure of resynchronization. Since infarction modulates electromechanical interactions, it also alters the mechanism of CRT. Bleeker et al. (Bleeker et al., 2006b) documented that patients with transmural posterolateral scar have a much lower response rate to CRT than those without scar, 14% vs. 81%. Increased scar volume has been found to result in unfavorable response to CRT in humans (Adelstein and Saba, 2007). Infarct location and scar transmurality are considered important (Choi et al., 2001; White et al., 2006) yet unknown factors that affect the relationship between electrical activation and contraction and contribute to diminished CRT efficacy.

Finally, the location of LV pacing has been shown to play an important role in CRT efficacy in patients (Butter et al., 2000; Helm et al., 2007; St John Sutton et al., 2003). Currently, LV pacing lead is implanted in a tributary of the coronary sinus, as in epicardial bi-V pacing in patients (Butter et al., 2001). However, for a small class of patients unsuitable for transvenous bi-V, a transseptal approach has been developed that allows endocardial bi-V pacing (Leclercq et al., 1999). Recent clinical evidence have brought to light the potential proarrhythmic effect of epicardial bi-V pacing (Fish et al., 2005), resulting from the reversal of the direction of electrical propagation in the LV. New findings indicate that endocardial bi-V pacing might be associated with improved resynchronization in canine models (Howard et al., 2011; van Deursen et al., 2009) and humans (Spragg et al., 2010). Thus determining the optimal location of LV pacing lead placement remains an open research question. Alternatively, recent clinical (Leclercq et al., 2008) and simulation (Niederer et al., 2012) results have demonstrated that multisite pacing, in which more than one pacing lead is placed at the LV, can better improve hemodynamic response to CRT compared with conventional bi-V pacing.

Multi-scale computational modeling of electromechanics in the normal and failing heart is now poised to address these open questions. Recent advancements in cardiac computational modeling, numerical algorithms and image processing techniques have enabled the development of detailed tomographically-reconstructed heart models that integrate functions from the molecular level to the electromechanical interactions in the intact organ. In this article, we employ such models to suggest potential approaches to optimizing CRT therapy. To achieve this goal, our research focuses on exploiting knowledge regarding the electromechanical delay in the heart as well as myocardial efficiency.

2. Electromechanical delay in the heart and how it can be used to optimize CRT

2.1. Significance of electromechanical delay

The time period between the local electrical depolarization and the onset of local myofiber shortening (mechanical activation) in the intact ventricles can last as much as tens of milliseconds. This electromechanical delay (EMD) is a function of the myocyte's intrinsic latent period between membrane depolarization and myofilament activation in the excitation-contraction process (Cordeiro et al., 2004), but is also dependent on the local myofiber mechanical loading conditions in the intact heart. Acute CRT therapy affects only the component of EMD that is due to the loading conditions, but has no influence on the cell-intrinsic E-C coupling latency (Russell et al., 2011). Thus, by understanding EMD and its distribution that is due to the loading conditions, one could suggest potential avenues for CRT optimization. Alternatively, since most echocardiography-based dyssynchrony measurements are affected by the timing of myofiber shortening onset, ascertaining the mechanisms underlying the EMD distribution may improve or lead to the development of novel indices of electromechanical dyssynchrony to identify potential CRT responders.

2.2. Electromechanical delay in the normal heart

The first computational study to assess the 3D distribution of EMD was by Usyk and McCulloch (Usyk and McCulloch, 2003). In this study, the authors employed an electromechanical model of the normal canine ventricles to determine the 3D EMD distribution during sinus rhythm and following LV pacing. With this early model, which in fact was the first whole-heart electromechanical model developed, the authors demonstrated that EMD may be both positive and negative, indicating that myofiber shortening may precede electrical activation in the whole heart. A more recent computational study by Gurev et al. (Gurev et al., 2010) have expounded on this work by providing thorough analysis of the 3D EMD distribution in the normal rabbit heart and its dependence on the loading conditions (i.e. on the electrical activation sequence). Simulations of electromechanical activity during sinus rhythm and LV epicardial pacing were conducted and compared to determine the effect of electrical activation pattern on the 3D distribution of EMD. The simulation results revealed that the 3D distribution of EMD was heterogeneous and depended on the electrical activation sequence. The distributions were markedly different for sinus rhythm and epicardial pacing. During sinus rhythm, the delay was longer at the epicardium compared to the endocardium and longer at the base compared to the apex. Following epicardial pacing, the distribution was markedly different: the posterior wall exhibited longer EMD compared to the anterior wall. Mechanistic analysis of the electromechanical behavior revealed that the late-depolarized regions were characterized with significant myofiber pre-stretch caused by the contraction of the early-depolarized regions. This pre-stretch, in turn, delayed myofiber shortening onset, and resulted in longer EMD there.

2.3. Assessment of EMD in DHF

The pumping inefficiency of the DHF heart arises from deleterious remodeling of cardiac electromechanical properties, from the sub-cellular to the organ level, and is thus expected to change the 3D EMD distribution. Determining the 3D EMD distribution in the setting of DHF and exploiting the mechanistic insight into the relation between electrical activation and mechanical contraction could offer clues to improvement in CRT delivery. In this section, we present our new image-based electromechanical model of the failing canine ventricles, and employ it to determine how the 3D distribution of EMD is altered in the setting of DHF.

A schematic of the electromechanical model of the failing heart is shown in Figure 1. Briefly, the electromechanical model is composed of two main components, an electrical and a mechanical component. The electrical component, which contains a biophysically-detailed representation of myocyte membrane kinetics, simulates the propagation of the action potential, while the mechanical component, which incorporates a biophysical model of myofilament dynamics, describes the active contraction and resultant deformation of the ventricles. The model is generic, and could be used with any geometry, image-based or idealized. The application of the model framework to MRI-based normal canine ventricular geometry is described in (Gurev et al., 2011). Details regarding the basics of the model generation, as well as the governing equations of each of the model components, can be found in (Gurev et al., 2011). We used the canine ventricular ionic model by Greenstein et al. (2006), and the model by Rice et al. (2008) to represent myofilament dynamics. The Rice et al. model (2008) was parameterized for the canine heart using electromechanical wave imaging data (Provost et al., 2010); the modified parameters can be found in that paper. The validation of the entire electromechanical model of the normal canine ventricles is also described in (Provost et al., 2010)

To develop the electromechanical model of the failing canine ventricles, the ventriclular geometry was generated from MR images of DHF canine ventricles (Fig.1), and the fiber and sheet architecture were constructed from DTMR images of the same DHF canine ventricles (both MR and DTMR data are publicly available (Helm et al.)), using the methodology by Gurev et al (2011). Using MR and DTMR images for the reconstruction of the DHF ventricles allows for the inclusion of the structural remodeling of the DHF ventricles.

To take into account the remodeling of the passive electromechanical tissue properties associated with DHF, the following changes were incorporated into the model (Fig. 1). First, electrical conductivities of the monodomain equations were reduced by 20% from the normal values (Roberts and Scher, 1982) to represent the slowed conduction in DHF (Akar et al., 2004). To account for the increased stiffness of the failing myocardial tissue as found experimentally (Wu et al., 2002), the passive stress scaling constant C in the strain–energy function (as described in (Usyk et al., 2000)) was increased fivefold. Finally, to incorporate deranged calcium handling associated with DHF (Aiba et al., 2009; O'Rourke et al., 1999), the peak amplitude and relaxation rate of the calcium transient function, which served as an input into the Rice et al (2008) model of the myofilament dynamics, was reduced to 70% and increased by 30% of the normal values, respectively. The normal values can be found in (Provost et al., 2010). Since CRT patients exhibit a left bundle branch block (LBBB) type of electrical activation, LBBB was simulated in both models by stimulating the endocardial surface at discrete locations as if the electrical activity was emanating from the activation of the corresponding branch of the Purkinje network.

Figure 2A presents the transmural electrical activation map in LBBB for the DHF heart in a short axis view; the same map for the normal canine heart but with LBBB is also shown.

This comparison allows the examination of the differences in electrical activation that arise from heart failure remodeling. In both hearts the depolarization wave travels from the right ventricular wall, through the septum and to the left ventricular lateral wall; the mechanical activation follows the same general direction (data not shown). The directions of electrical and mechanical wave propagation are consistent with previous animal results (Leclercq et al., 2002; Russell et al., 2011; van Deursen et al., 2009; Wyman et al., 2002). To assess the contribution of the detrimental remodeling associated with DHF to altering the 3D EMD distribution, the resultant transmural EMD maps for the normal and DHF hearts are compared in Figure 2B. The maps reveal that the 3D EMD distribution is heterogeneous in both the normal and failing hearts: the late-activated lateral wall is associated with an extended EMD as compared to the septum. However, in the DHF heart, EMD is longer that in the normal heart. The differences in EMD are particularly pronounced at the lateral wall (green in normal vs red in DHF, Figure 2B).

To further examine the relationship between electrical and mechanical activation in DHF, the electrical and mechanical activation times at 24 different locations in the left ventricular mid-wall in the normal and DHF canine ventricles are presented in Figure 2C. A linear regression analysis was performed. The slopes of the regression lines, which were obtained through least squares fitting, are greater than 1 in the normal and DHF hearts, indicating that the time interval between depolarization and onset of myofiber shortening is extended at the late-activated regions. However, this interval increases at a greater rate in the DHF heart (1.25 vs 1.63). These data demonstrate that the detrimental changes to the electromechanical properties in the DHF heart results in a prolonged EMD, particularly at the LV anterior wall during LBBB activation sequence.

2.4. Initial modeling efforts towards the assessment of contractile dyssynchrony and EMD in the infarcted heart

As mentioned in the Introduction (Section 1.1), the presence of MI is also expected to alter the EMD distribution in the ventricles. This section presents the initial modeling effort towards constructing an electromechanical model of the infarcted ventricles, which could be used to then assess the distribution of EMD in MI, and suggest possible improvements in CRT therapy in DHF patients with ischemic cardiomyopathy.

The model was reconstructed from MRI and DTMRI scans of canine ventricles with a 4-week old infarct. Briefly, the zone of infarct was segmented from the healthy myocardium using the fractional anisotropy values calculated from the DTMRI data, and the infarct zone was then divided into the akinetic scar and the partially viable peri-infarct using level set thresholding. Further details regarding the infarct segmentation can be found in Vadakkumpadan et al. (Vadakkumpadan et al., 2010). The mechanics finite elements mesh is shown in Figure 3A; the infarct zone (scar with peri-infarct), is demarcated in blue.

Because the scar is primarily composed of necrotic collagen, it was modeled as an insulator in the electrical component of the model. Based on the modeling work by Walker et al. (2005), the passive stress scaling constant C of the strain energy function was increased 1500% in the scar. No active tension was generated in the scar since collagen is not known to produce active tension. In the peri-infarct, the transverse electrical conductivity was reduced by 90% to reflect the 90% reduction in transverse gap junctional conductance as found experimentally (Yao et al., 2003). In accordance with previous modeling work (Sun et al., 2010; Walker et al., 2005), the peak active tension in the peri-infarct zone was reduced to 10% of its normal value and the passive stress scaling constant C of the strain energy function was increased fifteen fold.

An example simulation of paced propagation using the MRI-based electromechanical model of the infarcted canine ventricles is shown in Figure 3B. Owing to the tethering of the adjacent myocardium to the akinetic scar, myocyte shortening was impaired at the LV anterior wall, resulting in regional dyssynchrony. Adjacent regions of hypocontractility and normal contractility have been documented in previous animal studies (Ashikaga et al., 2005) as well as recent computational models of infarcted hearts (Kerckhoffs et al., 2009; Wenk et al., 2011). These data suggest that the EMD distribution in the MI heart will be markedly altered by the presence of an infarct; this distribution will depend on the specific scar location and transmurality. Electromechanical models with realistic topography of MI can be used to construct 3D maps of EMD for various scar locations and degrees of transmurality to reveal the mechanisms by which infarction alter the electromechanical activity of the heart.

2.5. Using the EMD distribution to guide CRT optimization

Suboptimal placement of the LV lead constitutes a major reason underlying the high non-response rate to CRT. To date, there is no clear consensus as to where to place the LV pacing lead to achieve optimal CRT response. Previous human studies (Ansalone et al., 2002; Howard et al., 2011; Suffoletto et al., 2006) have indicated that the site of latest electrical or the latest mechanical activation was associated with a greater hemodynamic benefit to CRT; however, recent human data (Derval et al., 2010; Fung et al., 2009; Spragg et al., 2010) suggests there is a lack of concordance between the site of latest electrical or mechanical activation and CRT response. In a pilot study (abstract) by Constantino et al. (Constantino et al., 2010), we proposed an alternative strategy to determine the LV pacing location in an effort to optimize the response to CRT: targeting the regions with the longest EMD. This section presents simulation results towards optimization of CRT employing this strategy. Using the image-based model of canine DHF electromechanics, as in Section 2.4, CRT was delivered by pacing at the RV apex, with the LV pacing electrode placed at 18 different epicardial sites along the LV free wall. For each LV pacing site, response to CRT was assessed by calculating the percent change in maximal rise in LV pressure (dP/dt_{max}) as compared to that in the DHF heart.

Using the transmural EMD maps that were constructed in Section 2.4, the region with the longest EMD was determined to be the endocardial surface of the lateral wall between the base and the mid-ventricles during LBBB. Figure 4A presents CRT response as a function of LV pacing location. The baseline dP/dtmax was 901 mmHg/s, consistent with reported experiment values (Leclercq et al., 2002). Maximal hemodynamic benefit occurred when the LV pacing site was located near the base and mid-ventricle, which was within the region of longest EMD. Although the distribution of optimal pacing locations differs, values in dP/dt max improvement in following CRT were consistent with those found in canine experiments (Helm et al., 2007; Strik et al., 2012). The relationship between LV pacing location and longest EMD region is quantified in Figure 4B. For each pacing site, CRT response and the longitudinal distance between the pacing site and the center of the region with the longest EMD were plotted. Increase in dP/dt max strongly correlated with the longitudinal distance between LV pacing site and the center of the region with longest EMD ($r=-.86$, $p<0.05$).

These computational results demonstrate that targeting the region with the longest EMD results in greatest hemodynamic response to CRT. Thus determining the 3D EMD distribution in DHF could be used to guide the optimal placement of the LV pacing electrode for CRT. It remains to be determined whether the same approach will be applicable in the infarcted heart, where discord between electrical and mechanical activity is exacerbated by the presence of the infarct (Ashikaga et al., 2005).

3. Using energy consumption as a guide to CRT optimization

An alternative approach to identify the optimal LV pacing location for CRT may be to target the LV location that results in maximum increase in myocardial efficiency while simultaneously minimizing the heterogeneity in energy consumption. This suggestion is based on the fact that myocardial efficiency, the ratio of mechanical work performed by the ventricles to myocardial energy consumption, is markedly reduced in DHF patients (Suga, 1990). Furthermore, it has been shown that CRT improves myocardial efficiency in DHF patients (Lindner et al., 2006). Since current experimental techniques are limited by the inability to record local mechanical activity and energy consumption in the ventricles with high spatiotemporal resolution, subject-specific electromechanical models of the DHF ventricles that incorporate a biophysically-detailed representation of cardiac myofilament dynamics can be employed to analyze the effect of CRT on local energy consumption and total myocardial efficiency in the setting of DHF and potentially identify the optimal LV pacing location. Below we present such results.

Simulations of LBBB and CRT were performed using the MRI-based electromechanical model of DHF canine heart, as in Sections 2.2 and 2.3. The use of the Rice et al. (Rice et al., 2008) representation of myofilament dynamics allowed for the calculation of local energy consumption. ATP consumption distribution was calculated by integrating over time the ATP consumption rate, a function of the ATP-consuming cross-bridge detachment rate and the single overlap fraction of thick filaments. The ATP consumption of the entire ventricle was then determined by spatially integrating the local ATP consumption throughout the entire ventricular volume, as done in our previous publication (Lim et al., 2012). Finally, mechanical work was calculated by integrating the area within the pressure-volume loop generated by the model, and myocardial efficiency was calculted as the ratio of mechanical work to total ATP consumption in the ventricles.

Consistent with findings in patients(Lindner et al., 2006; Lindner et al., 2005; Ukkonen et al., 2003), CRT resulted in improvement in myocardial efficiency (Figure 5A). This stems from the fact that CRT increased the mechanical work performed by the ventricles without increasing the total ventricular energy consumption. Although total energy consumption was unaltered, CRT homogenized energy consumption throughout the ventricles by increasing energy consumption at the septum and reducing it at the lateral wall (Figure 5B); this finding is consistent with experimental data (Lindner et al., 2006; Lindner et al., 2005; Ukkonen et al., 2003). These results demonstrate that computational models of DHF electromechanics can accurately simulate the effects of CRT on myocardial efficiency and local energy consumption and can be used to determine the LV pacing location that minimizes the heterogeneity in energy consumption and maximizes myocardial efficiency.

4. Limitations

Representation of the papillary muscles was not included in the electromechanical models. Incorporating the papillary muscles may affect the longitudinal deformation, which in turn could alter the EMD and energy consumption distribution. Another limitation is the assumption of homogeneous calcium handling properties throughout the myocardium in the DHF heart. Recent experimental data (Aiba et al., 2009; Chakir et al., 2009) has demonstrated that changes to calcium handling differ at the lateral and anterior wall in the DHF canine heart, which may affect the distribution of EMD and energy consumption. Future studies are needed to address these effects on the 3D distribution of EMD and energy consumption.

5. Conclusions

A comprehensive characterization of the spatiotemporal electromechanical interactions in the DHF heart, without and with MI, is fundamental to the effort towards improving CRT efficacy. This paper demonstrates that a biophysically-based model of ventricular electromechanics that incorporates representations from the scale of the protein to the intact organ is a powerful methodology to provide insight into the electromechanical interactions in the heart. More importantly, this paper highlights how the basic science insight into the electromechanical activity of the DHF heart gained from computational modeling can be exploited to guide improvements in CRT delivery. The simulation results presented here indicate that optimal CRT strategy in the DHF heart can be achieved by pacing at the LV location characterized with longest EMD. The same approach can be used to determine whether CRT can be also optimized by targeting the region with the longest EMD in the infarcted heart. In addition, computational modeling could also aid in the identification of the LV pacing location that results in maximal myocardial efficiency and most beneficial regional energy consumption. With new advancements in computational modeling and increased ubiquity of computers in the clinic, it will not be long before electromechanical models of DHF patients' hearts that are enriched with patient-specific data will serve as a bedside tool for diagnosis and treatment planning.

Acknowledgments

This work was supported by National Institutes of Health (NIH) grant R01-HL103428, National Science Foundation Grants CBET-0933029 and IOS-1124804 to NAT, and by NIH fellowship F31-HL103090 to JLC.

References

Abraham WT, Fisher WG, Smith AL, Delurgio DB, Leon AR, Loh E, Kocovic DZ, Packer M, Clavell AL, Hayes DL, Ellestad M, Trupp RJ, Underwood J, Pickering F, Truex C, McAtee P, Messenger J. Cardiac resynchronization in chronic heart failure. N Engl J Med. 2002; 346:1845–53. [PubMed: 12063368]

Adelstein EC, Saba S. Scar Burden by Myocardial Perfusion Imaging Predicts Echocardiographic Response to Cardiac Resynchronization Therapy in Ischemic Cardiomyopathy. Am Heart J. 2007; 153:105–12. [PubMed: 17174647]

Aiba T, Hesketh GG, Barth AS, Liu T, Daya S, Chakir K, Dimaano VL, Abraham TP, O'Rourke B, Akar FG, Kass DA, Tomaselli GF. Electrophysiological consequences of dyssynchronous heart failure and its restoration by resynchronization therapy. Circulation. 2009; 119:1220–30. [PubMed: 19237662]

Akar FG, Nass RD, Hahn S, Cingolani E, Shah M, Hesketh GG, DiSilvestre D, Tunin RS, Kass DA, Tomaselli GF. Dynamic Changes in Conduction Velocity and Gap Junction Properties During Development of Pacing-Induced Heart Failure. Am J Physiol Heart Circ Physiol. 2007; 293:H1223–30. [PubMed: 17434978]

Akar FG, Spragg DD, Tunin RS, Kass DA, Tomaselli GF. Mechanisms Underlying Conduction Slowing and Arrhythmogenesis in Nonischemic Dilated Cardiomyopathy. Circ Res. 2004; 95:717–25. [PubMed: 15345654]

Ansalone G, Giannantoni P, Ricci R, Trambaiolo P, Fedele F, Santini M. Doppler myocardial imaging to evaluate the effectiveness of pacing sites in patients receiving biventricular pacing. J Am Coll Cardiol. 2002; 39:489–99. [PubMed: 11823088]

Ashikaga H, Mickelsen SR, Ennis DB, Rodriguez I, Kellman P, Wen H, McVeigh ER. Electromechanical analysis of infarct border zone in chronic myocardial infarction. Am J Physiol Heart Circ Physiol. 2005; 289:H1099–105. [PubMed: 15908463]

Auricchio A, Stellbrink C, Block M, Sack S, Vogt J, Bakker P, Klein H, Kramer A, Ding J, Salo R, Tockman B, Pochet T, Spinelli J. Effect of Pacing Chamber and Atrioventricular Delay on Acute Systolic Function of Paced Patients with Congestive Heart Failure. The Pacing Therapies for

Congestive Heart Failure Study Group. The Guidant Congestive Heart Failure Research Group. Circulation. 1999; 99:2993–3001. [PubMed: 10368116]

Bax JJ, Bleeker GB, Marwick TH, Molhoek SG, Boersma E, Steendijk P, van der Wall EE, Schalij MJ. Left Ventricular Dyssynchrony Predicts Response and Prognosis after Cardiac Resynchronization Therapy. J Am Coll Cardiol. 2004; 44:1834–40. [PubMed: 15519016]

Beshai JF, Grimm RA, Nagueh SF, Baker JH, Beau SL, Greenberg SM, Pires LA, Tchou PJ. Cardiac-resynchronization therapy in heart failure with narrow QRS complexes. N Eng J Med. 2007; 357:2461–2471.

Bleeker GB, Bax JJ, Steendijk P, Schalij MJ, van der Wall EE. Left Ventricular Dyssynchrony in Patients with Heart Failure: Pathophysiology, Diagnosis and Treatment. Nat Clin Pract Cardiovasc Med. 2006a; 3:213–9. [PubMed: 16568130]

Bleeker GB, Kaandorp TA, Lamb HJ, Boersma E, Steendijk P, de Roos A, van der Wall EE, Schalij MJ, Bax JJ. Effect of Posterolateral Scar Tissue on Clinical and Echocardiographic Improvement after Cardiac Resynchronization Therapy. Circulation. 2006b; 113:969–76. [PubMed: 16476852]

Butter C, Auricchio A, Stellbrink C, Fleck E, Ding J, Yu Y, Huvelle E, Spinelli J. Effect of Resynchronization Therapy Stimulation Site on the Systolic Function of Heart Failure Patients. Circulation. 2001; 104:3026–9. [PubMed: 11748094]

Butter C, Auricchio A, Stellbrink C, Schlegl M, Fleck E, Horsch W, Huvelle E, Ding J, Kramer A. Should Stimulation Site Be Tailored in the Individual Heart Failure Patient? Am J Cardiol. 2000; 86:144K–151K.

Byrne MJ, Helm RH, Daya S, Osman NF, Halperin HR, Berger RD, Kass DA, Lardo AC. Diminished left ventricular dyssynchrony and impact of resynchronization in failing hearts with right versus left bundle branch block. J Am Coll Cardiol. 2007; 50:1484–90. [PubMed: 17919569]

Chakir K, Daya SK, Aiba T, Tunin RS, Dimaano VL, Abraham TP, Jaques-Robinson KM, Lai EW, Pacak K, Zhu WZ, Xiao RP, Tomaselli GF, Kass DA. Mechanisms of enhanced beta-adrenergic reserve from cardiac resynchronization therapy. Circulation. 2009; 119:1231–40. [PubMed: 19237665]

Cheng A, Nguyen TC, Malinowski M, Daughters GT, Miller DC, Ingels NB. Heterogeneity of left ventricular wall thickening mechanisms. Circulation. 2008; 118:713–721. [PubMed: 18663088]

Choi KM, Kim RJ, Gubernikoff G, Vargas JD, Parker M, Judd RM. Transmural Extent of Acute Myocardial Infarction Predicts Long-Term Improvement in Contractile Function. Circulation. 2001; 104:1101–7. [PubMed: 11535563]

Chung ES, Leon AR, Tavazzi L, Sun JP, Nihoyannopoulos P, Merlino J, Abraham WT, Ghio S, Leclercq C, Bax JJ. Results of the Predictors of Response to CRT (PROSPECT) trial. Circulation. 2008; 117:2608–2616. [PubMed: 18458170]

Constantino J, Gurev V, Trayanova N. Optimal cardiac resynchronization therapy is achieved by pacing from the LV region with the longest electromechanical delay. Heart Rhythm. 2010; 7:S164–165.

Cordeiro JM, Greene L, Heilmann C, Antzelevitch D, Antzelevitch C. Transmural heterogeneity of calcium activity and mechanical function in the canine left ventricle. Am J Physiol Heart Circ Physiol. 2004; 286:H1471–9. [PubMed: 14670817]

Derval N, Steendijk P, Gula LJ, Deplagne A, Laborderie J, Sacher F, Knecht S, Wright M, Nault I, Ploux S, Ritter P, Bordachar P, Lafitte S, Reant P, Klein GJ, Narayan SM, Garrigue S, Hocini M, Haissaguerre M, Clementy J, Jais P. Optimizing hemodynamics in heart failure patients by systematic screening of left ventricular pacing sites: the lateral left ventricular wall and the coronary sinus are rarely the best sites. J Am Coll Cardiol. 2010; 55:566–75. [PubMed: 19931364]

Fauchier L, Marie O, Casset-Senon D, Babuty D, Cosnay P, Fauchier JP. Interventricular and Intraventricular Dyssynchrony in Idiopathic Dilated Cardiomyopathy: A Prognostic Study with Fourier Phase Analysis of Radionuclide Angioscintigraphy. J Am Coll Cardiol. 2002; 40:2022–30. [PubMed: 12475464]

Fauchier L, Marie O, Casset-Senon D, Babuty D, Cosnay P, Fauchier JP. Reliability of QRS Duration and Morphology on Surface Electrocardiogram to Identify Ventricular Dyssynchrony in Patients with Idiopathic Dilated Cardiomyopathy. Am J Cardiol. 2003; 92:341–4. [PubMed: 12888151]

Fish JM, Brugada J, Antzelevitch C. Potential Proarrhythmic Effects of Biventricular Pacing. J Am Coll Cardiol. 2005; 46:2340–7. [PubMed: 16360069]

Fung JW, Lam YY, Zhang Q, Yip GW, Chan WW, Chan GC, Chan JY, Yu CM. Effect of left ventricular lead concordance to the delayed contraction segment on echocardiographic and clinical outcomes after cardiac resynchronization therapy. J Cardiovasc Electrophysiol. 2009; 20:530–5. [PubMed: 19054250]

Greenstein JL, Hinch R, Winslow RL. Mechanisms of excitation-contraction coupling in an integrative model of the cardiac ventricular myocyte. Biophys J. 2006; 90:77–91. [PubMed: 16214852]

Gurev V, Constantino J, Rice JJ, Trayanova NA. Distribution of electromechanical delay in the heart: insights from a three-dimensional electromechanical model. Biophys J. 2010; 99:745–54. [PubMed: 20682251]

Gurev V, Lee T, Constantino J, Arevalo H, Trayanova NA. Models of cardiac electromechanics based on individual hearts imaging data: image-based electromechanical models of the heart. Biomech Model Mechanobiol. 2011; 10:295–306. [PubMed: 20589408]

Helm, PA.; Winslow, RL.; McVeigh, E. Dtmri Data Sets Center for Cardiovascular Bioinformatics and Modeling. http://gforge.icm.jhu.edu/gf/project/dtmri_data_sets/

Helm PA, Younes L, Beg MF, Ennis DB, Leclercq C, Faris OP, McVeigh E, Kass D, Miller MI, Winslow RL. Evidence of Structural Remodeling in the Dyssynchronous Failing Heart. Circ Res. 2006; 98:125–32. [PubMed: 16339482]

Helm RH, Byrne M, Helm PA, Daya SK, Osman NF, Tunin R, Halperin HR, Berger RD, Kass DA, Lardo AC. Three-Dimensional Mapping of Optimal Left Ventricular Pacing Site for Cardiac Resynchronization. Circulation. 2007; 115:953–61. [PubMed: 17296857]

Helm RH, Leclercq C, Faris OP, Ozturk C, McVeigh E, Lardo AC, Kass DA. Cardiac Dyssynchrony Analysis Using Circumferential Versus Longitudinal Strain: Implications for Assessing Cardiac Resynchronization. Circulation. 2005; 111:2760–7. [PubMed: 15911694]

Hooks DA, Trew ML, Caldwell BJ, Sands GB, LeGrice IJ, Smaill BH. Laminar Arrangement of Ventricular Myocytes Influences Electrical Behavior of the Heart. Circ Res. 2007; 101:e103–12. [PubMed: 17947797]

Howard EJ, Covell JW, Mulligan LJ, McCulloch AD, Omens JH, Kerckhoffs RC. Improvement in pump function with endocardial biventricular pacing increases with activation time at the left ventricular pacing site in failing canine hearts. Am J Physiol Heart Circ Physiol. 2011; 301:H1447–55. [PubMed: 21784986]

Kaab S, Nuss HB, Chiamvimonvat N, O'Rourke B, Pak PH, Kass DA, Marban E, Tomaselli GF. Ionic Mechanism of Action Potential Prolongation in Ventricular Myocytes from Dogs with Pacing-Induced Heart Failure. Circ Res. 1996; 78:262–73. [PubMed: 8575070]

Kerckhoffs RC, McCulloch AD, Omens JH, Mulligan LJ. Effects of Biventricular Pacing and Scar Size in a Computational Model of the Failing Heart with Left Bundle Branch Block. Med Image Anal. 2009; 13:362–9. [PubMed: 18675578]

Kerckhoffs RC, Omens JH, McCulloch AD, Mulligan LJ. Ventricular dilation and electrical dyssynchrony synergistically increase regional mechanical nonuniformity but not mechanical dyssynchrony: a computational model. Circ Heart Fail. 2011; 3:528–36. [PubMed: 20466849]

Leclercq C, Faris O, Tunin R, Johnson J, Kato R, Evans F, Spinelli J, Halperin H, McVeigh E, Kass DA. Systolic improvement and mechanical resynchronization does not require electrical synchrony in the dilated failing heart with left bundle-branch block. Circulation. 2002; 106:1760–3. [PubMed: 12356626]

Leclercq C, Gadler F, Kranig W, Ellery S, Gras D, Lazarus A, Clementy J, Boulogne E, Daubert JC. A randomized comparison of triple-site versus dual-site ventricular stimulation in patients with congestive heart failure. J Am Coll Cardiol. 2008; 51:1455–62. [PubMed: 18402900]

Leclercq F, Hager FX, Macia JC, Mariottini CJ, Pasquie JL, Grolleau R. Left Ventricular Lead Insertion Using a Modified Transseptal Catheterization Technique: A Totally Endocardial Approach for Permanent Biventricular Pacing in End-Stage Heart Failure. Pacing Clin Electrophysiol. 1999; 22:1570–5. [PubMed: 10598958]

LeGrice IJ, Takayama Y, Covell JW. Transverse Shear Along Myocardial Cleavage Planes Provides a Mechanism for Normal Systolic Wall Thickening. Circ Res. 1995; 77:182–93. [PubMed: 7788876]

Lim KM, Constantino J, Gurev V, Zhu R, Shim EB, Trayanova NA. Comparison of the effects of continuous and pulsatile left ventricular-assist devices on ventricular unloading using a cardiac electromechanics model. J Physiol Sci. 2012; 62:11–9. [PubMed: 22076841]

Linde C, Leclercq C, Rex S, Garrigue S, Lavergne T, Cazeau S, McKenna W, Fitzgerald M, Deharo JC, Alonso C, Walker S, Braunschweig F, Bailleul C, Daubert JC. Long-term benefits of biventricular pacing in congestive heart failure: results from the MUltisite STimulation in cardiomyopathy (MUSTIC) study. J Am Coll Cardiol. 2002; 40:111–8. [PubMed: 12103264]

Lindner O, Sorensen J, Vogt J, Fricke E, Baller D, Horstkotte D, Burchert W. Cardiac efficiency and oxygen consumption measured with 11C-acetate PET after long-term cardiac resynchronization therapy. J Nucl Med. 2006; 47:378–83. [PubMed: 16513605]

Lindner O, Vogt J, Kammeier A, Wielepp P, Holzinger J, Baller D, Lamp B, Hansky B, Korfer R, Horstkotte D, Burchert W. Effect of cardiac resynchronization therapy on global and regional oxygen consumption and myocardial blood flow in patients with non-ischaemic and ischaemic cardiomyopathy. Eur Heart J. 2005; 26:70–6. [PubMed: 15615802]

Lloyd-Jones D, Adams R, Carnethon M, De Simone G, Ferguson TB, Flegal K, Ford E, Furie K, Go A, Greenlund K, Haase N, Hailpern S, Ho M, Howard V, Kissela B, Kittner S, Lackland D, Lisabeth L, Marelli A, McDermott M, Meigs J, Mozaffarian D, Nichol G, O'Donnell C, Roger V, Rosamond W, Sacco R, Sorlie P, Stafford R, Steinberger J, Thom T, Wasserthiel-Smoller S, Wong N, Wylie-Rosett J, Hong Y. Heart Disease and Stroke Statistics-2009 Update: A Report from the American Heart Association Statistics Committee and Stroke Statistics Subcommittee. Circulation. 2009; 119:480–6. [PubMed: 19171871]

Marijianowski MM, Teeling P, Mann J, Becker AE. Dilated Cardiomyopathy Is Associated with an Increase in the Type I/Type III Collagen Ratio: A Quantitative Assessment. J Am Coll Cardiol. 1995; 25:1263–72. [PubMed: 7722119]

Miyazaki C, Redfield MM, Powell BD, Lin GM, Herges RM, Hodge DO, Olson LJ, Hayes DL, Espinosa RE, Rea RF, Bruce CJ, Nelson SM, Miller FA, Oh JK. Dyssynchrony indices to predict response to cardiac resynchronization therapy: a comprehensive prospective single-center study. Circ Heart Fail. 2010; 3:565–73. [PubMed: 20647479]

Nelson GS, Berger RD, Fetics BJ, Talbot M, Spinelli JC, Hare JM, Kass DA. Left Ventricular or Biventricular Pacing Improves Cardiac Function at Diminished Energy Cost in Patients with Dilated Cardiomyopathy and Left Bundle-Branch Block. Circulation. 2000; 102:3053–9. [PubMed: 11120694]

Niederer SA, Shetty AK, Plank G, Bostock J, Razavi R, Smith NP, Rinaldi CA. Biophysical modeling to simulate the response to multisite left ventricular stimulation using a quadripolar pacing lead. Pacing Clin Electrophysiol. 2012; 35:204–14. [PubMed: 22040178]

O'Rourke B, Kass DA, Tomaselli GF, Kaab S, Tunin R, Marban E. Mechanisms of Altered Excitation-Contraction Coupling in Canine Tachycardia-Induced Heart Failure, I: Experimental Studies. Circ Res. 1999; 84:562–70. [PubMed: 10082478]

Pitzalis MV, Iacoviello M, Romito R, Massari F, Rizzon B, Luzzi G, Guida P, Andriani A, Mastropasqua F, Rizzon P. Cardiac Resynchronization Therapy Tailored by Echocardiographic Evaluation of Ventricular Asynchrony. J Am Coll Cardiol. 2002; 40:1615–22. [PubMed: 12427414]

Provost J, Gurev V, Trayanova N, Konofagou EE. Mapping of cardiac electrical activation with electromechanical wave imaging: an in silico-in vivo reciprocity study. Heart Rhythm. 2010; 8:752–9. [PubMed: 21185403]

Rice JJ, Wang F, Bers DM, de Tombe PP. Approximate model of cooperative activation and crossbridge cycling in cardiac muscle using ordinary differential equations. Biophys J. 2008; 95:2368–90. [PubMed: 18234826]

Roberts DE, Scher AM. Effect of tissue anisotropy on extracellular potential fields in canine myocardium in situ. Circ Res. 1982; 50:342–51. [PubMed: 7060230]

Russell K, Smiseth OA, Gjesdal O, Qvigstad E, Norseng PA, Sjaastad I, Opdahl A, Skulstad H, Edvardsen T, Remme EW. Mechanism of prolonged electromechanical delay in late activated

myocardium during left bundle branch block. Am J Physiol Heart Circ Physiol. 2011; 301:H2334–43. [PubMed: 21984549]

Spragg DD, Dong J, Fetics BJ, Helm R, Marine JE, Cheng A, Henrikson CA, Kass DA, Berger RD. Optimal left ventricular endocardial pacing sites for cardiac resynchronization therapy in patients with ischemic cardiomyopathy. J Am Coll Cardiol. 2010; 56:774–81. [PubMed: 20797490]

St John Sutton MG, Plappert T, Abraham WT, Smith AL, DeLurgio DB, Leon AR, Loh E, Kocovic DZ, Fisher WG, Ellestad M, Messenger J, Kruger K, Hilpisch KE, Hill MR. Effect of Cardiac Resynchronization Therapy on Left Ventricular Size and Function in Chronic Heart Failure. Circulation. 2003; 107:1985–90. [PubMed: 12668512]

Strik M, Rademakers LM, van Deursen CJ, van Hunnik A, Kuiper M, Klersy C, Auricchio A, Prinzen FW. Endocardial left ventricular pacing improves cardiac resynchronization therapy in chronic asynchronous infarction and heart failure models. Circ Arrhythm Electrophysiol. 2012; 5:191–200. [PubMed: 22062796]

Suffoletto MS, Dohi K, Cannesson M, Saba S, Gorcsan J 3rd. Novel speckle-tracking radial strain from routine black-and-white echocardiographic images to quantify dyssynchrony and predict response to cardiac resynchronization therapy. Circulation. 2006; 113:960–8. [PubMed: 16476850]

Suga H. Ventricular energetics. Physiol Rev. 1990; 70:247–77. [PubMed: 2181496]

Sun K, Zhang Z, Suzuki T, Wenk JF, Stander N, Einstein DR, Saloner DA, Wallace AW, Guccione JM, Ratcliffe MB. Dor procedure for dyskinetic anteroapical myocardial infarction fails to improve contractility in the border zone. J Thorac Cardiovasc Surg. 2010; 140:233–9. 239, e1–4. [PubMed: 20299030]

Sutton MG, Plappert T, Hilpisch KE, Abraham WT, Hayes DL, Chinchoy E. Sustained Reverse Left Ventricular Structural Remodeling with Cardiac Resynchronization at One Year Is a Function of Etiology: Quantitative Doppler Echocardiographic Evidence from the Multicenter Insync Randomized Clinical Evaluation (MIRACLE). Circulation. 2006; 113:266–72. [PubMed: 16401777]

Ukkonen H, Beanlands RS, Burwash IG, de Kemp RA, Nahmias C, Fallen E, Hill MR, Tang AS. Effect of cardiac resynchronization on myocardial efficiency and regional oxidative metabolism. Circulation. 2003; 107:28–31. [PubMed: 12515738]

Usyk TP, Mazhari R, McCulloch AD. Effect of Laminar Orthotropic Myofiber Architecture on Regional Stress and Strain in the Canine Left Ventricle. J. Elasticity. 2000; 61:143–164.

Usyk TP, McCulloch AD. Relationship between Regional Shortening and Asynchronous Electrical Activation in a Three-Dimensional Model of Ventricular Electromechanics. J Cardiovasc Electrophysiol. 2003; 14:S196–202. [PubMed: 14760924]

Vadakkumpadan F, Arevalo H, Prassl AJ, Chen J, Kickinger F, Kohl P, Plank G, Trayanova N. Image-based models of cardiac structure in health and disease. Wiley Interdiscip Rev Syst Biol Med. 2010; 2:489–506. [PubMed: 20582162]

van Deursen C, van Geldorp IE, Rademakers LM, van Hunnik A, Kuiper M, Klersy C, Auricchio A, Prinzen FW. Left ventricular endocardial pacing improves resynchronization therapy in canine left bundle-branch hearts. Circ Arrhythm Electrophysiol. 2009; 2:580–7. [PubMed: 19843927]

Walker JC, Ratcliffe MB, Zhang P, Wallace AW, Fata B, Hsu EW, Saloner D, Guccione JM. MRI-Based Finite-Element Analysis of Left Ventricular Aneurysm. Am J Physiol Heart Circ Physiol. 2005; 289:H692–700. [PubMed: 15778283]

Wenk JF, Sun K, Zhang Z, Soleimani M, Ge L, Saloner D, Wallace AW, Ratcliffe MB, Guccione JM. Regional left ventricular myocardial contractility and stress in a finite element model of posterobasal myocardial infarction. J Biomech Eng. 2011; 133:044501. [PubMed: 21428685]

White JA, Yee R, Yuan X, Krahn A, Skanes A, Parker M, Klein G, Drangova M. Delayed Enhancement Magnetic Resonance Imaging Predicts Response to Cardiac Resynchronization Therapy in Patients with Intraventricular Dyssynchrony. J Am Coll Cardiol. 2006; 48:1953–60. [PubMed: 17112984]

Wu Y, Bell SP, Trombitas K, Witt CC, Labeit S, LeWinter MM, Granzier H. Changes in Titin Isoform Expression in Pacing-Induced Cardiac Failure Give Rise to Increased Passive Muscle Stiffness. Circulation. 2002; 106:1384–9. [PubMed: 12221057]

Wyman BT, Hunter WC, Prinzen FW, Faris OP, McVeigh ER. Effects of single- and biventricular pacing on temporal and spatial dynamics of ventricular contraction. Am J Physiol Heart Circ Physiol. 2002; 282:H372–9. [PubMed: 11748084]

Yao JA, Hussain W, Patel P, Peters NS, Boyden PA, Wit AL. Remodeling of gap junctional channel function in epicardial border zone of healing canine infarcts. Circ Res. 2003; 92:437–43. [PubMed: 12600896]

Yu CM, Chau E, Sanderson JE, Fan K, Tang MO, Fung WH, Lin H, Kong SL, Lam YM, Hill MR, Lau CP. Tissue Doppler Echocardiographic Evidence of Reverse Remodeling and Improved Synchronicity by Simultaneously Delaying Regional Contraction after Biventricular Pacing Therapy in Heart Failure. Circulation. 2002; 105:438–45. [PubMed: 11815425]

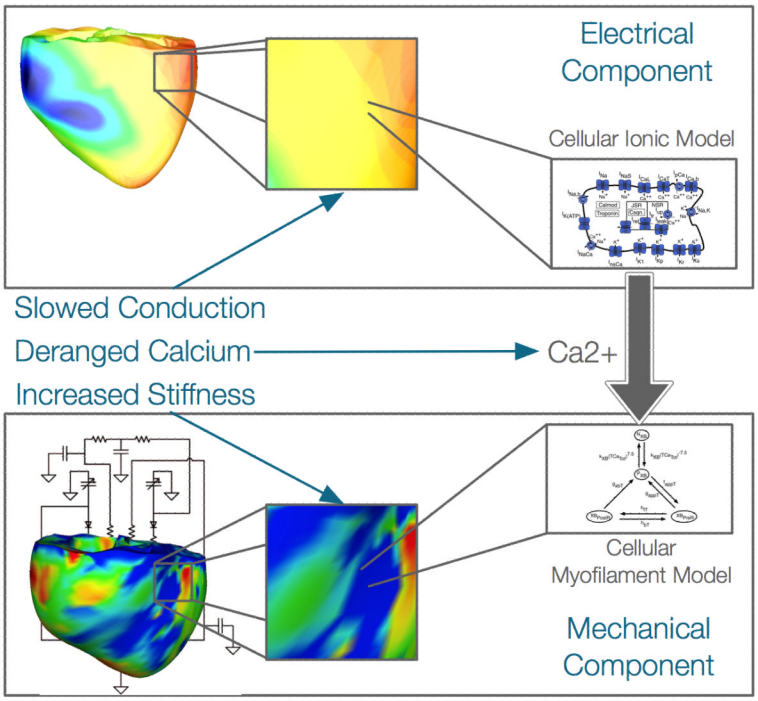

Figure 1.
Overall approach to image-based modeling of DHF electromechanics. The geometrical images of hearts in the electrical and mechanical components are of the remodeled DHF canine heart. The light blue arrows indicate where the remodeling aspects of slowed conduction, deranged calcium, increased stiffness were incorporated into the model.

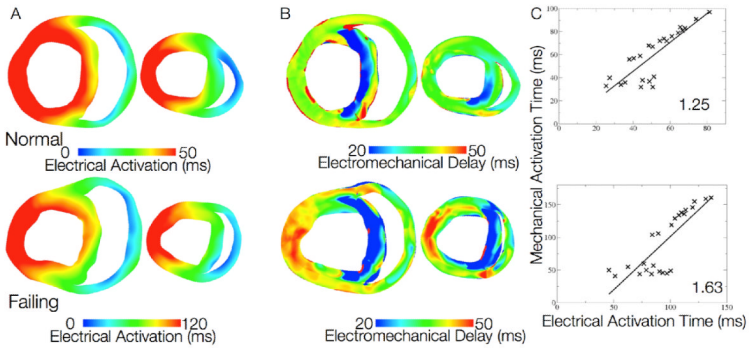

Figure 2.

A. Transmural short-axis electrical maps during LBBB for normal (upper) and DHF (lower) hearts **B.** Transmural short-axis EMD maps during LBBB for normal (upper) and DHF (lower) hearts. In each map, the anterior and posterior walls are at the top and bottom, respectively **C.** Correlation between electrical activation and mechanical activation time during LBBB for normal (upper) and DHF (lower) hearts.

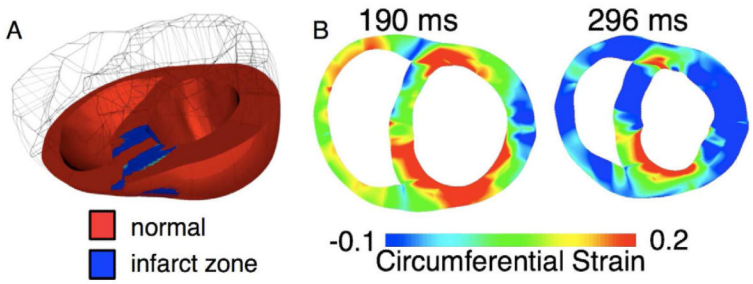

Figure 3.

A. Computational mesh for the mechanical component of the MRI-based electromechanical model of post-MI canine heart. The infarct zone (scar with peri-infarct) is demarcated in blue. **B.** Transmural distribution of fiber strain during sinus rhythm at two instants of time. Reference state is the unloaded state. The color scale is saturated.

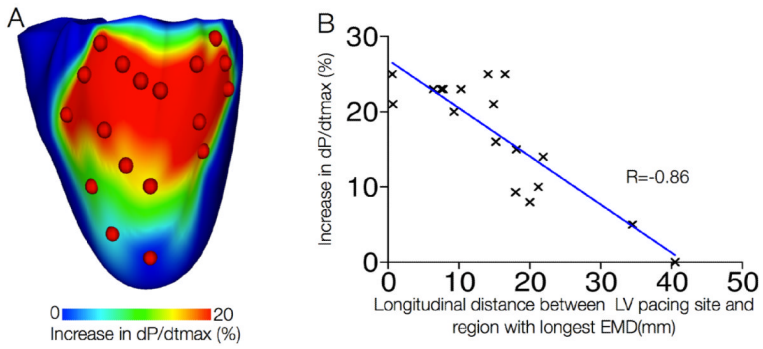

Figure 4.

A. Map of the percentage increase in dP/dt_{max} as a function of the LV pacing site. Red dots denote LV pacing sites. **B** Correlation of longitudinal distance between LV pacing site and region with longest EMD, and percentage increase in dP/dt_{max}.

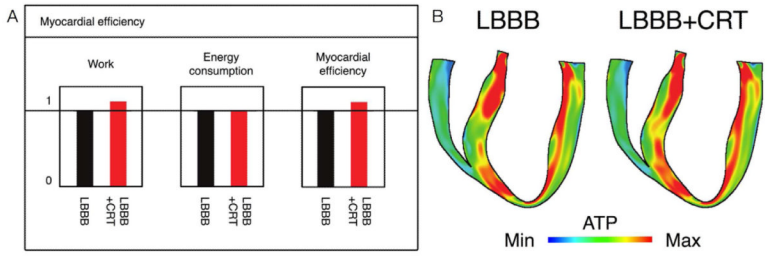

Figure 5.

A. Bar graph of stroke work (left), total ventricular energy consumption (middle) and myocardial efficiency (right) during LBBB and following CRT. Values are normalized to LBBB (baseline) values. **B** Distribution of ATP consumption during LBBB and following CRT.